2019 2nd IEEE International Conference on Soft Robotics (RoboSoft)
COEX, Seoul, Korea, April 14-18, 2019

# ConTact Sensors: A Tactile Sensor Readily Integrable into Soft Robots

Pornthep Preechayasomboon[1] and Eric Rombokas[1,2]

***Abstract*— In this paper, we propose a soft robotics sensor that uses multiple modalities of sensing, fluid pressure and electrical resistance, of a single conductive fluid medium. Each modality responds differently to the same stimulus, allowing richer sensing than two distinct sensors would provide. We embody this concept into ConTact Sensor, a soft tactile sensor that can detect the force and contact length of the object compressing it. ConTact Sensor shares similar fabrication materials as most soft robotic designs, thus it can be combined with soft actuators or even embodied into a soft actuator itself. We detail the design, fabrication and characterization of ConTact Sensor and provide an example of integrating the sensor in a liquid-filled PneuNets actuator.**

## I. Introduction

Control in soft robotics has primarily relied on open-loop control. This can be forgiving in some use cases, such as a soft robotic gripper that takes advantage of its natural compliance. In some cases, such as robotic walkers, a simple open-loop replay is enough to control the robot for a certain performance envelope [1]. In more complex scenarios, such as dexterous manipulation or robots that interact with the environment, the dynamics are unpredictable and control is more difficult, and would greatly benefit from having feedback [2][3].

However, some soft robots rely on external feedback which often results in limitations in environments and work volumes. For example, a snake-like robot that relies on optical trackers cannot be used in confined or visually occluding spaces, an environment in which it would definitely excel in. One concept to solve this issue is to embed exclusive structures designed for sensing in the robot, such as resistive flex sensors [4], and hall effect sensors [5]. However, this form of feedback comes at the cost of a mismatch between stiffnesses of the sensor and the robot, therefore any sensors built into the robot must themselves be soft.

Another approach is to integrate softer materials to be used as sensors. Some integrated sensors are based on elastomers built into the soft robot that include channels for liquid-phase materials [6]. The elastomer layers are patterned with channels for gallium alloys [7], designed so that when the channel shape changes, a desired physical property (e.g. curvature of the robot) is sensed. Similarly, optical channels can be used to detect deformation of the waveguide, and to relate that change to the state of the robot [8]. More recently, embedded 3D printing was used to integrate multiple distinct sensors of different properties (curvature, contact, inflation, etc.) into the same pneumatically-actuated soft robotic system [9].

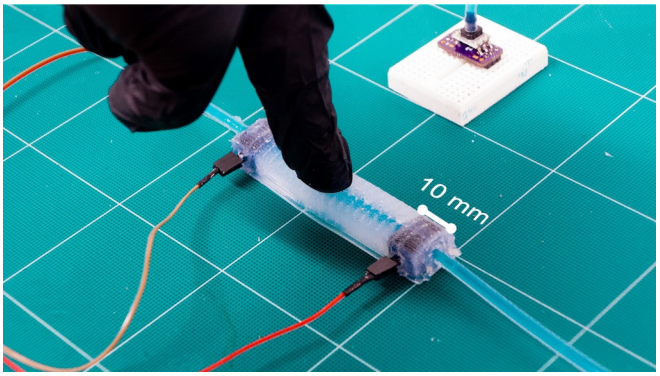


Fig. 1. ConTact Sensor being used as a tactile sensor to determine the force and contact length of an experimenter's fingertip. The name ConTact is from the main principle of sensing: a Conductive fluid, and the sensor itself being a Tactile sensor.

In this paper, we describe a means for sensing more than one dynamic characteristic of the fluid medium, namely the electrical resistance and fluid pressure of a conductive hydraulic fluid. We propose an embodiment of the concept as a tactile sensor design that is able to discern between a range of physical depressions from light to heavy and from small to large that is able to be integrated into most existing soft robot designs due to its similarity in materials and construction.

## II. Design

In its essence, ConTact Sensor is ionic solution housed in a deformable tube. The sensed quantities are the changes in internal pressure and the changes in the electrical resistance of the fluid, which according to the resistivity formula ($R = \frac{\rho L}{A}$), the resistance (R) given a constant resistivity ($\rho$), depends on the length (L) and cross-sectional area (A) of the medium. If the sensor is pressed into or pinched, the cross sectional area would decrease leading to an increase in electrical resistance. The resistance also varies with the amount of length-wise area being affected. And in both cases, the overall fluid pressure in the sensor increases. Using this duality of sensing characteristics, we can derive richer sensing capabilities from a single structure.

### A. Sensing Mechanism

Since the sensor can be thought as a simple tube of conductive fluid, we can create an approximate model for the behavior of the sensor under loading. First, we can estimate the deformation of the cross-section as a shape with

[1]**rombolabs**, Department of Mechanical Engineering, University of Washington, Seattle, WA, USA. Email: prnthp@uw.edu, Website: prnthp.github.io
[2]RR&D Center for Limb Loss and MoBility (CLiMB), VA Puget Sound Health Care System, Seattle, WA, USA. Email: rombokas@uw.edu, Website: rombolabs.github.io

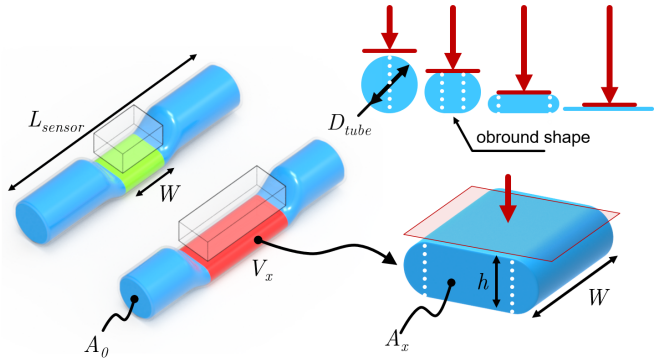


Fig. 2. The geometric representation of ConTact Sensor's chamber under deformation from two different indenters.

constant circumference due to the incompressibility of the hyperelastic silicone rubber. In other words, when the tube is being compressed, the circumference of the tube remains constant, beginning with a circle, then transitioning into an obround shape and ending with a collapsed line, as shown in Fig. 2. By approximating the shape as an obround, the area of the cross-section can then be described as:

$$A_x = (D_{tube} - h)\frac{\pi h}{2} + \frac{\pi h^2}{4} \tag{1}$$

Then, if the width of the loaded area is $W$, the volume of the portion of the tube under load is simply the width multiplied by the cross-sectional area:

$$V_x = W A_x \tag{2}$$

Under load, the pressure in the sensor increases, however, the increase in pressure is shared between both fluids in the sensor: the conductive liquid and the remaining dissolved and trapped air in the sensor. With this fact in mind and treating the conductive liquid as an incompressible fluid and the air as an ideal gas, we can model the behavior of the pressure increase under load with Boyle's law $P_1V_1 = P_2V_2$, where we assume the volumetric displacement of the liquid exclusively effects the pressure and volume of the compressible air:

$$P = \frac{P_0V_0}{(V_0 - V_x)} = \frac{P_0V_0}{V_0 - WA_x} \tag{3}$$

As for the resistance of the conductive fluid, we can model it as a continuum of conductive material using the resistivity formula $R = \rho\frac{L}{A}$. We simplify the model by discretizing the volume into two parts, the deformed volume, directly affected by an indenter, and the remaining undeformed volume, as shown in Fig. 2 and arrive at the following model for resistance:

$$R_{total} = \rho\left[\frac{L_{sensor} - W}{A_0} + \frac{W}{A_x}\right] \tag{4}$$

We plot the effect of the deformation amount, in deformed height $h$ with pressure and resistance of various indenter widths $W$ in Fig. 3. The two examples of indenter widths

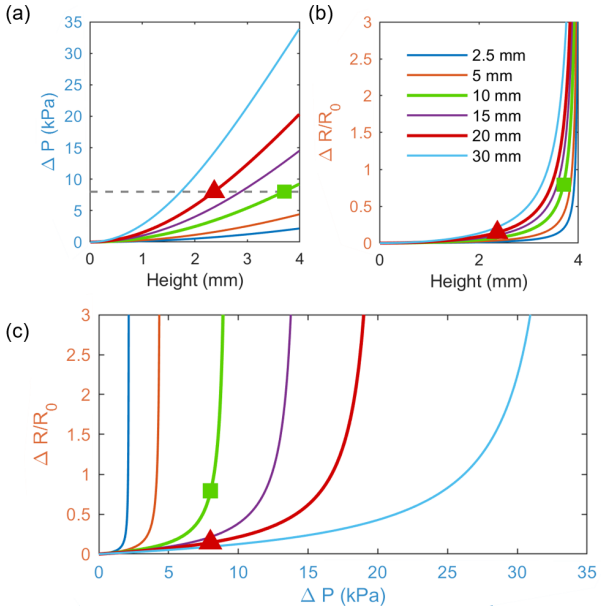


Fig. 3. Theoretical sensor responses to being pressed with various sized indenters. The markers represent the state of indenters of two different widths (10 mm and 20 mm), each at different heights of deformation. The two indenters would have the same pressure readings, but significantly different resistance readings, therefore we can distinguish between the two at any height, given enough deformation and sensor resolution.

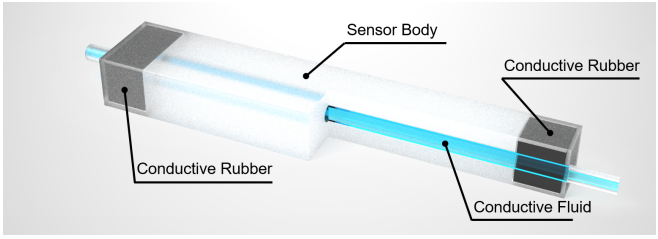


Fig. 4. ConTact Sensor's components in a cross-section view. The sensor body is depicted as cut away at the halfway point for better visualization of the conductive fluid channel.

in Fig. 2 are also plot in Fig. 3. The dashed line and markers in Fig. 3 (a) represents the same resulting pressure reading from the two different indenters if the smaller 10 mm indenter is pressed in almost fully while the larger 20 mm indenter is pressed in approximately halfway. However, since the resulting resistance readings, shown in Fig. 3 (b), are significantly different, we can discern between the two indenters at any height when using both modalities, as shown in Fig. 3 (c).

## III. Fabrication

ConTact Sensor is designed to be readily integrable into traditional silicone-based soft robots therefore the sensor is primarily fabricated from casting soft silicone elastomer (Platsil Gel-25, Polytek Development Corp.) in a plastic mold. An electrically conductive interface is required between the measurement equipment and the fluid to obtain the electrical resistance. However, simply inserting electrical wires to contact the fluid through the elastomer would cer-

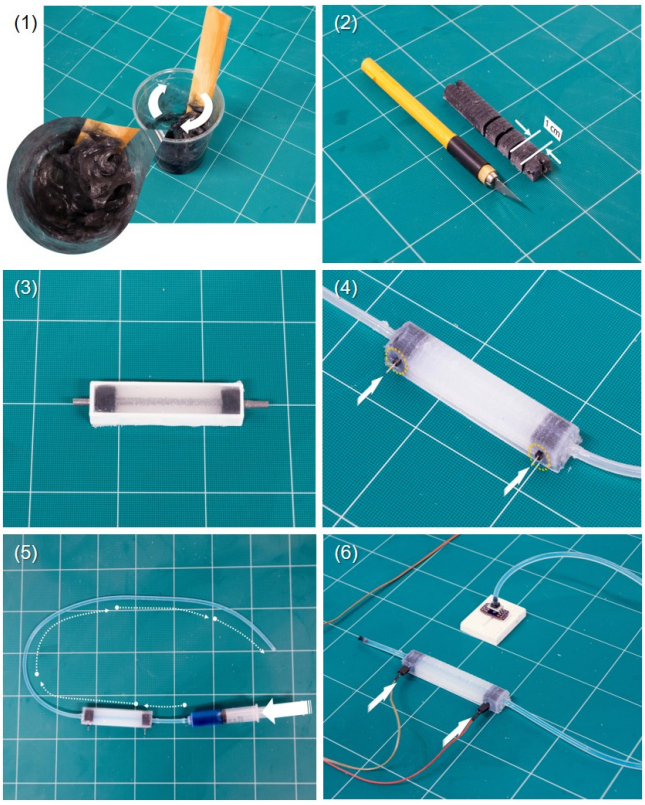


Fig. 5. Overview of the steps for fabricating ConTact Sensor, as numbered; 1. Preparing the conductive silicone rubber 2. Cutting the conductive rubber into 10 mm long sections 3. Casting the main body of the sensor with the conductive rubber in-line with the metal rod. 4. Adding copper leads to the sensor. 5. Filling the sensor with salt water dyed with food coloring. 6. Attaching ConTact Sensor to the data acquisition system.

tainly be prone to leakages [10], therefore conductive silicone fabricated from silicone elastomer and chopped carbon fibers is used as the interface. Since the conductive silicone is made from the same type of elastomer as the body, the sensor's fluids are sealed from the outside environment and the sensor is significantly less prone to leakage. Another benefit of using conductive silicone rubber is reducing the transition between low-stiffness materials e.g. the silicone rubber and fluids to high-stiffness materials e.g. the copper wires, which should improve the mechanical robustness of the sensor.

ConTact Sensors can be produced in any shape and size as long as three main components are present: the main sensor body, the conductive rubber ends, and the ionic solution, as shown in Fig. 4. For this proof of concept we fabricated a main sensor body in a brick-like shape, 16 mm wide by 10 mm tall by 85 mm in length, with a 4 mm diameter tubular section spanning the length of the whole body. The conductive rubber ends, which conduct electrical current between the internal fluid and the exterior, are 10 mm long rectangular sections with a 4 mm hole embedded in the sensor's body at each end. The ionic solution is simply saline solution with 5 parts table salt to 95 parts plain water by weight (5 %wt NaCl).

The fabrication of ConTact Sensor can be divided into three main steps: casting the conductive silicone ends, casting the sensor body and filling the sensor prior to use. A comprehensive guide to fabricating ConTact Sensors is also available at the Soft Robotics Toolkit website. A brief overview of all the steps involved is shown in Fig. 5 and the following are the fabrication steps in detail and reasoning behind them.

### A. Conductive Silicone Rubber

Commercially available conductive silicone elastomer are often propriety mixes of silicone rubber with graphite particles, which have long cure-times and less than ideal mechanical properties. [11] The conductive silicone rubber in ConTact Sensor is made by mixing 5 mm long carbon fiber strands (.125" Chopped Carbon, Innovative Composite Technologies) with two-part platinum-cure silicone rubber (Platsil Gel-25, Polytek Development Corp.). The resulting carbon fiber and silicone rubber mixture cures just as fast as the bare silicone rubber and the cured conductive rubber is compliant and not brittle. The method was first published by Andrew Quitmeyer on the Instructables website [12].

Casting the conductive silicone rubber for one ConTact Sensor starts with soaking 0.5 g of chopped carbon fiber strands in 1 g of 70 % isopropanol, which is just enough to wet the strands and disperse them. The wet strands are then either left to partially dry or squeezed to remove the excess alcohol. The strands are then vigorously stirred into a mixture of 20 g of Part A and 20 g of Part B of the silicone rubber. The carbon fiber-silicone rubber mixture's conductivity can be verified at this step using an ohmmeter. The ratio of 0.5 g to 40 g silicone elastomer was found empirically through trial-and-error and has desirable viscosity for casting and adequate electrical conductivity —in the order of several hundred Ohms in resistance across 10 mm. Increasing the amount of carbon fiber strands can decrease the overall resistance at the cost of higher viscosity, which could lead to problems during pouring and casting. Before casting, a 4 mm diameter metal rod is inserted into the mold and finally the now paste-like mixture is spread into the mold. The metal rod serves to displace the volume that would become the 4 mm inner channel of the sensor. A minimum time of one hour is required for the room temperature vulcanization (RTV) of the rubber to complete. Once the rubber has dried, an ohmmeter is used to verify the electrical resistance of the conductive rubber. The conductive rubber is then removed from the mold and cut into 10 mm long sections.

### B. Sensor Body

ConTact Sensor's main body is cast from a similar platinum-cure silicone rubber (Plat-Sil Gel 10, Polytek Development Corp.) to the conductive rubber by using the same mold. The conductive ends are positioned in a metal rod within the mold. Then, the silicone rubber is simply poured into the open-top mold and left to vulcanize. Once the rubber has dried, the metal rod is removed leaving a 4 mm diameter hollow section throughout the sensor. To complete the sensor, two 4 mm silicone tubes with an inner diameter of 2 mm (PUTC4, MiSUMi Group Inc.) are glued

in place with silicone adhesive. (Sil-Poxy, Smooth-On, Inc.) The same adhesive is used to hold copper pins that have been pierced into the conductive rubber in place. Note that the silicone adhesive is only for holding the pins in place, and does not serve any purpose to seal the sensor.

### C. Conductive Fluid

The conductive fluid used in the ConTact Sensors presented in this paper is 5% saline solution or 5 wt% Sodium Chloride (NaCl). The solution is prepared by weighing 5 grams of table salt (The Kroger Co.) followed by 95 grams of room temperature tap water. Food coloring (The Kroger Co.) is added to make the fluid visible through the semi-transparent silicone rubber and tubing.

Alternative ionic fluids, such as 1-ethyl-3-methyl imidazolium ethylsulfate (EMIM-ES) or salt dissolved in glycerin [10][13][14], could possibly be used, but salt water is trivial to acquire and prepare. A lower concentration akin to medicinal saline (0.9% w/v) could also be used for ConTact Sensors in contact with humans as it is considered roughly isotonic to human cells [15].

As we are measuring the fluid's electrical resistance, one major drawback of using salt water as the conductive fluid is the solution is ionic, which means that the resistance cannot be measured with the standard method of applying a DC voltage and measuring the voltage drop. Applying a DC voltage across two leads in salt water will cause the positive ions ($Na^+$) to pool on the negative lead and negative ions ($Cl^-$) to pool on the positive lead, causing a charge buildup which gives an erroneous reading of the resistance.

In this paper, we use alternating current (AC) to measure the electrical resistance. Using our data acquisition system (USB-6251, National Instruments) we apply a 1 volt peak-to-peak sinusoidal waveform centered at 0 volts across the ConTact Sensor and a known resistance in a voltage divider configuration as shown in Fig. 6. The resistance of the fluid inside the sensor can then be calculated as (5).

$$R_{ConTact} = R_{known} \times \frac{V_M}{V_S - V_M} \tag{5}$$

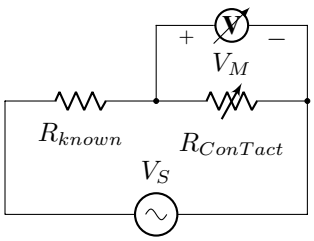


Fig. 6. The voltage divider circuit used for measuring the salt water with a sinusoidal waveform.

## IV. Sensor Characterization

### A. Material Properties

The carbon fiber based conductive silicone rubber had a volume resistivity ranging from 750 to 2460 $\Omega \cdot m$ across 6 different batches with an average of 1340 $\Omega \cdot m$. However, the overall resistance of each distinctly shaped sample remained near 150 Ω. We hypothesize that the conductivity of the silicone is from the random orientation of carbon fiber strands creating a network of conductive paths propagating throughout the silicone rubber.

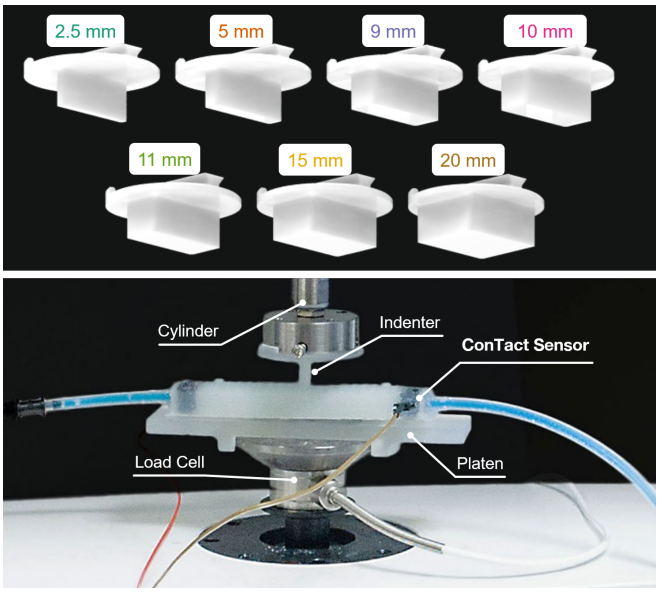


Fig. 7. Top: Indenters with their widths printed directly above, color coded to match subsequent plots in this paper. Bottom: ConTact Sensor is placed on a 3D printed platen that is mounted on a load cell. The material testing machine's cylinder is fitted with a 3D printed indenter. The background has been artificially darkened for clarity.

### B. Experimental Methods

We performed a series of indentation experiments in order to calibrate and characterize the sensor. The sensor was placed on a custom platen on a universal testing machine (ElectroForce 3200, TA Instruments). The universal testing machine is designed for testing soft and compliant specimens using forces lower than 200 N. The platen is mounted on top of a load cell (WMC-50, Interface Inc.). The setup can be seen in Fig. 7 The cylinder of the testing machine is fitted with indenters of various widths and shapes ranging from 2.5 mm to 20 mm in width.

The sensor's conductive rubber ends were connected to our data acquisition system. One end of the silicone tubing was connected to a pressure sensor (ABPMANT100PG2A3, Honeywell) that interfaces via $I^2C$ with a microcontroller (Teensy 3.5, PJRC) and the other end was capped shut. We performed all data logging using LabVIEW (National Instruments) software to record the fluid electrical resistance, pressure, force from the loadcell and indenter displacement.

Each experiment consists of moving the indenter down to a depth of 5.5 mm, starting directly on top of the sensor, with a fixed speed of 2 mm/s, then dwelling for three seconds and finally lifting up to its starting position.

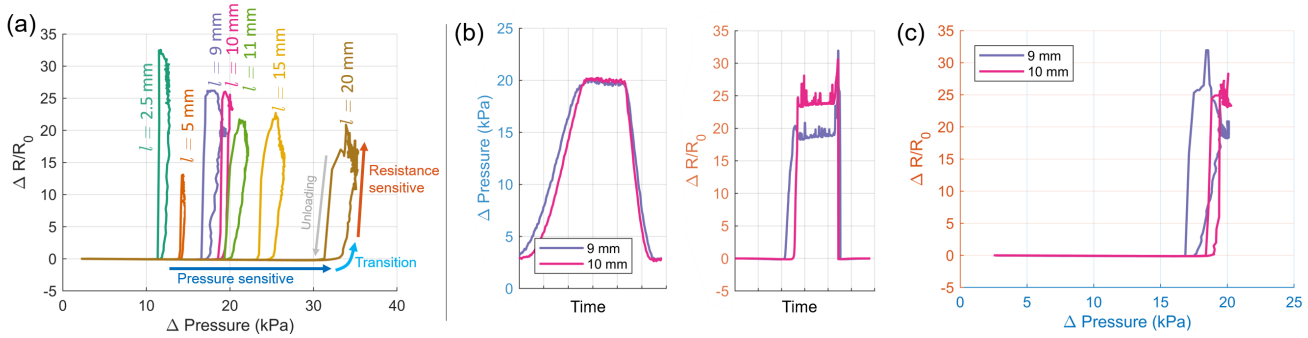


Fig. 8. ConTact Sensor's response to various indentation sizes and forces. (a) Plot showing the color-coded raw responses to indenters shown in Fig. 7. The sensor shows a transition of behavior from responding in pressure increase to responding in resistance increase. (b) Plots showing almost identical pressure mode response (left) for different sized indenters, but significantly different response in resistance mode (right). (c) The same data from (b) when plotted in a Pressure-Resistance plane.

### C. Experimental Results

We performed 5 indentation trials per indenter with a total of 7 indenters, totalling 35 trials. We preprocessed the data by truncating the data stream for each indentation to right before the indenter starts moving down and right after the indenter returns to its starting position. (∼12 seconds) The data was collected at a sampling frequency of 50 Hz. The sensor's electrical resistance data in voltages was fed through a third order median filter and then converted to Ohms using (5) with $R_{known}$ set to 20 $k\Omega$. The resistance was then scaled to the starting resistance of each trial and zeroed, achieving $\Delta R/R_0$ as shown in subsequent plots. Displacement, pressure and force data was simply scaled to their pre-calibrated values and then zeroed to each trial.

As shown in Fig. 8 (a), when plotting the electrical resistance ($\Delta R/R_0$) against the fluid pressure ($\Delta P$), the sensor clearly responds differently to each size indenter. As the indenter starts loading into the sensor, at first the pressure increases, after a certain point the resistance also increases, at a faster rate, and remains stable when the indenter has reached its lowest position. This behavior is akin to the behavior described in Section II.A, where the resistance barely shows any response during the "pressure sensitive" period, but rapidly catches up during the "transition" period which is just prior to the pressure saturating. It can be observed from Fig. 8 (b) and (c) that with pressure data alone, the sensor cannot discern between a 9 mm and 10 mm indenter.

### D. Estimation

Using data only from the duration of the downstroke of the indentation experiments, we fit a linear regression model to the pressure and resistance data to predict the force acting on the sensor. We used MATLAB's `fitlm` to perform linear regression using ordinary least squares weighting and allowing for interactions between input variables. The resulting model (6) predicts the force to within an average of 12.28 N of the actual force, which is approximately 10% of the full dynamic range, as shown in Fig. 9 (b).

$$F = k_r R + k_p P + k_i RP + k_{r2} R^2 + k_{p2} P^2 \tag{6}$$

Looking at the sensor response in Fig. 8 (a), for each sized indenter, the sensor's resistance rapidly increases at different pressures. As per the sensor's design, we used the resistance and an empirically derived threshold as an activation function for the pressure. In other words, the contact length is zero until a certain resistance is reached, and then the contact length is the pressure scaled by some value. Using the model, we can estimate the contact length to within 0.429 mm of the actual length, as shown in Fig. 9 (c).

$$L = (k_l P + L_0) \times 1(R \geq R_{thresh})$$
$$1(R \geq R_{thresh}) = \begin{cases} 1, & R \geq R_{thresh} \\ 0, & R < R_{thresh} \end{cases} \tag{7}$$

## V. Application

As a demonstration of ConTact Sensor's ability to be integrated into soft robotic designs, we embedded one into the tip of a PneuNets Actuator, as shown in Fig. 10 (a). We designed the actuator with the intention of having the sensor in the same hydraulic circuit as the actuator, i.e. the actuation fluid passes through the sensor during inflation and deflation. The actuation fluid was 5%wt salt water, prepared in the same manner as mentioned in the previous sections. To achieve the complex geometry, the actuator was cast using lost-wax casting.

We performed a series of experiments by pressing the sensor against six indenters from Fig. 7 (sizes 2.5 mm, 5 mm, 9 mm, 10 mm, 11 mm and 15 mm). The results show that the embedded ConTact Sensor can discern between different sized indenters, as shown in Fig. 10 (c). The overall response is similar to the results in the previous section, but a linearized model of the response is more difficult to derive. It should be noted that our current model does not yet account for actuation and we expect to expand this result in the near future and apply learning-based predictions in place of the regression.

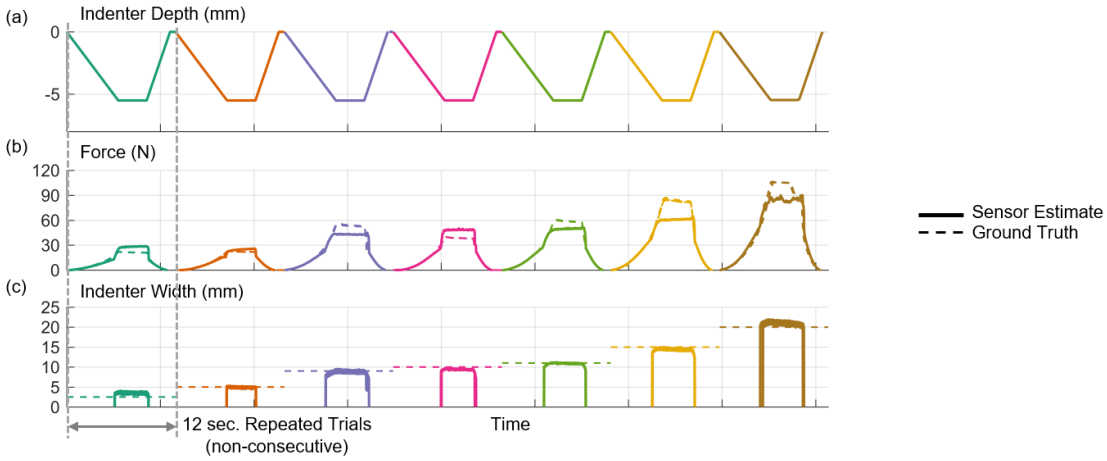


Fig. 9. Plots showing the force and contact length estimation derived from the sensor readings. Each section represents a different width indenter. (a) Plot of the indenter's depth into into the sensor (b) Plot of the force estimation and ground truth. (c) Plot of the contact length estimation and ground truth.

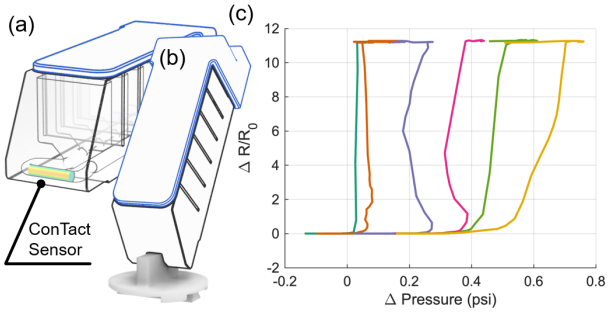


Fig. 10. ConTact Sensor's response when embedded in the tip of a modified PneuNets Actuator. The sensor can discern small from large contact lengths.

## VI. Conclusion & Future Work

Arguably, the ConTact Sensor is simple in concept and design. However, the sensor's simplicity enables it to be integrated into other soft robotic designs, especially those with liquid-based actuation. We presented a novel method of sensing force and contact area by using a single fluid medium and the overall concept of using more than one physical characteristic of sensing medium to achieve richer sensing.

Future work will be on expanding the modes of sensing, as of now ConTact Sensor primarily responds to normal force, but with complex geometries of the inner channel we hope to be able to measure tangential force (shear force). As discussed in the previous section, the sensor output is more challenging to interpret when it is integrated with a PneuNets actuator. We will continue to refine the design until full proprioception is achieved.

## Acknowledgement

The authors would like to thank Chris Richburg and Matt Kindig (Center for Limb Loss and MoBility (CLiMB), VA Puget Sound, Seattle, WA, USA) and members of Rombolabs for their help. We would also like to thank the Soft Robotics Toolkit for creating a platform for soft robotics developers to share their findings in an instructive and accessible way.

## References

[1] H. Wang, M. Totaro, and L. Beccai, "Toward Perceptive Soft Robots: Progress and Challenges," 2018.

[2] C. Della Santina, R. K. Katzschmann, A. Bicchi, and D. Rus, "Dynamic control of soft robots interacting with the environment," in *IEEE International Conference on Soft Robotics, RoboSoft 2018*, Livorno, Italy, 2018, pp. 46–53.

[3] M. T. Gillespie, C. M. Best, E. C. Townsend, D. Wingate, and M. D. Killpack, "Learning Nonlinear Dynamic Models of Soft Robots for Model Predictive Control with Neural Networks," in *IEEE International Conference on Soft Robotics (RoboSoft)*, Livorno, Italy, 2018, pp. 39–45.

[4] K. Elgeneidy, N. Lohse, and M. Jackson, "Bending angle prediction and control of soft pneumatic actuators with embedded flex sensors – A data-driven approach," *Mechatronics*, 2018.

[5] Y. Yang, Y. Chen, Y. Li, Z. Wang, and Y. Li, "Novel Variable-Stiffness Robotic Fingers with Built-In Position Feedback," *Soft Robotics*, 2017.

[6] D. Rus and M. T. Tolley, "Design, fabrication and control of soft robots," *Nature*, vol. 521, p. 467, 5 2015.

[7] D. M. Vogt, Y. Park, and R. J. Wood, "Design and Characterization of a Soft Multi-Axis Force Sensor Using Embedded Microfluidic Channels," *IEEE Sensors Journal*, vol. 13, no. 10, pp. 4056–4064, 2013.

[8] H. Zhao, K. O 'brien, S. Li, and R. F. Shepherd, "Optoelectronically innervated soft prosthetic hand via stretchable optical waveguides," *Science Robotics*, vol. 7529, no. 1, p. eaai7529, 2016.

[9] R. L. Truby, M. Wehner, A. K. Grosskopf, D. M. Vogt, S. G. Uzel, R. J. Wood, and J. A. Lewis, "Soft Somatosensitive Actuators via Embedded 3D Printing," *Advanced Materials*, 2018.

[10] J. T. Muth, D. M. Vogt, R. L. Truby, Y. Mengüç, D. B. Kolesky, R. J. Wood, and J. A. Lewis, "Embedded 3D printing of strain sensors within highly stretchable elastomers," *Advanced Materials*, 2014.

[11] K. G. Princy, R. Joseph, and C. S. Kartha, "Studies on conductive silicone rubber compounds," *Journal of Applied Polymer Science*, 1998.

[12] Andrew Quitmeyer, "Silc Circuits: High Performance Conductive Silicone," p. 1, 2015. [Online]. Available: https://www.instructables.com/id/Silc-Circuits-High-Performance-Conductive-Silicone/

[13] J. B. Chossat, Y. L. Park, R. J. Wood, and V. Duchaine, "A soft strain sensor based on ionic and metal liquids," *IEEE Sensors Journal*, 2013.

[14] K. Noda, E. Iwase, K. Matsumoto, and I. Shimoyama, "Stretchable liquid tactile sensor for robot-joints," in *IEEE International Conference on Robotics and Automation*, Anchorage, Alaska, USA, 2010, pp. 4212–4217.

[15] S. Russo, T. Ranzani, H. Liu, S. Nefti-Meziani, K. Althoefer, and A. Menciassi, "Soft and Stretchable Sensor Using Biocompatible Electrodes and Liquid for Medical Applications," *Soft Robotics*, 2015.